Available online at www.sciencedirect.com

ScienceDirect

Procedia IUTAM 9 (2013) 69 – 78

Procedia IUTAM

www.elsevier.com/locate/procedia

IUTAM Symposium on Understanding Common Aspects of Extreme Events in Fluids

On the singular nature of turbulent boundary layers

J.C. Klewicki[a,b]

[a] *University of New Hampshire, Department of Mechanical Engineering, Durham 03824, USA*
[b] *University of Melbourne, Department of Mechanical Engineering, Melbourne 3010, Australia*

Abstract

An estimate is derived for the rate at which, with increasing Reynolds number, the vorticity in turbulent boundary layers is confined to a diminishing fraction of the overall flow domain. For laminar boundary layers this rate is reflected in the self-similar coordinate stretching that determines the Reynolds number scalings for boundary layer growth and skin friction. For the turbulent boundary layer this rate is shown to also derive from an underlying similarity structure. An accounting of the magnitude ordering of terms in the mean dynamical equation for the turbulent boundary layer reveals a four layer structure. This structure forms during the transitional regime, persists for all subsequent Reynolds numbers, and provides a framework for describing the evolution of the boundary layer vorticity and momentum fields. Multiscale analyses that exploit the four layer ordering reveal that two kinds of self-similarities are formally admitted. With increasing Reynolds number, these are shown to be associated with two kinds of scale-separation between the motions characteristic of the velocity and vorticity fields. One pertains to the near-wall spatial confinement of the vorticity field owing to vorticity stretching, and the other pertains to the advective transport of decreasingly smaller scale vortical motions over a domain that approaches the overall flow width as the Reynolds number becomes large. The scalings associated with the self-similar structure indicate that slightly greater than 50% of the total vorticity content is, with increasing Reynolds number, confined to a near-wall layer of diminishing thickness, with the remainder attributable to a domain that approaches the total layer thickness. Within the larger domain at least 50% of the vorticity is concentrated in narrow vortical fissures that also decrease in relative scale with Reynolds number. Spanwise vorticity measurements in laboratory boundary layers and the atmospheric surface layer are shown to be in agreement with the theoretical predictions, but also provide evidence that at sufficiently high Reynolds number, the vortical fissures develop an intermittent internal structure. Collectively, these results indicate that, on average at any given instant, at least 75% of the boundary layer circulation (per unit length) is confined to a region that diminishes like $\log(\delta^+)/\sqrt{\delta^+}$ as the boundary layer Reynolds number, $\delta^+ = \delta u_\tau/\nu \to \infty$.

Selection and peer-review under responsibility of the School of Mathematical Sciences, University College Dublin

Keywords: turbulent boundary layers; asymptotic behavior; wall-flow vorticity

1. Introduction

The existence of a region near a no-slip surface within which the direct effects of viscosity are dynamically significant constitutes a definitional attribute of boundary layer structure (laminar, transitional, or turbulent). From an

* J. C. Klewicki. Tel.: +01-603-862-3113 ; fax: +01-603-862-1865.
E-mail address: joe.klewicki@unh.edu

Selection and peer-review under responsibility of the School of Mathematical Sciences, University College Dublin
doi:10.1016/j.piutam.2013.09.007

examination of the vorticity form of the Navier-Stokes equation, this region also coincides with non-negligible vorticity. As the Reynolds number (say $\delta^+ = \delta u_\tau/\nu$) increases, this region occupies a decreasing fraction of the overall flow domain. This physically describes how the solution to the Navier-Stokes equation approaches that of the Euler equation as $\delta^+ \to \infty$, with the associated conceptual model for the boundary layer being a vortex sheet positioned infinitesimally above the wall. The purpose of the present study is to provide a description of how this process occurs in the turbulent boundary layer over a smooth surface.

The analysis applies to statistically stationary incompressible turbulent boundary layer flow with zero streamwise pressure gradient. The main flow is in the x direction, with the wall-normal direction denoted by y. Upper case letters or angle brackets denote time-averaged quantities, lower case letters indicate fluctuations about the mean, instantaneous quantities are denoted by a tilde, and a prime denotes the rms of a fluctuating quantity. The x, y and z velocity components are given by variants of u, v and w, respectively. Vorticity component directions are denoted by their subscript, δ is used to denote the boundary layer thickness, and U_∞ is the freestream velocity. The friction velocity is given by $u_\tau = \sqrt{\tau_w/\rho}$, where τ_w is the mean wall shear stress and ρ is the mass density. The dynamic and kinematic viscosities are respectively denoted by μ, and $\nu = \mu/\rho$. Quantities normalized by ν and u_τ are denoted by a superscript $+$. The Reynolds number is given by $\delta^+ = \delta u_\tau/\nu$, and the small parameter, ε, by $\varepsilon = 1/\sqrt{\delta^+}$. Circulation per unit length is denoted by Γ.

A brief examination of steady zero pressure gradient boundary layer flow in the laminar regime provides a useful context for highlighting the practical and theoretical significances of this issue. The relevant differential statement of dynamics for this flow is

$$\tilde{u}\frac{\partial \tilde{u}}{\partial x} + \tilde{v}\frac{\partial \tilde{u}}{\partial y} = \nu\frac{\partial^2 \tilde{u}}{\partial y^2}, \tag{1}$$

which indicates that the time rate of change of streamwise momentum is affected by a retarding viscous force. To within the boundary layer approximation, $\tilde{\omega}_z \simeq -\partial\tilde{u}/\partial y$, and thus the outward spread of momentum deficit identically coincides with a wall-normal gradient of $\tilde{\omega}_z$. Also in accord with boundary layer concepts, (1) constitutes the leading order approximation to the Navier-Stokes equations for laminar flow over a flat no-slip surface as the Reynolds number (generally defined as $R_x = U_\infty x/\nu$, where x is measured from the leading edge) tends to infinity. When combined with the continuity equation and relevant boundary conditions, (1) forms a well-posed boundary value problem that formally admits the similarity solution first demonstrated by Blasius, e.g., see [1]. Important to the present purpose, the scalings embodied in the coordinate transformations associated with this similarity solution describe the rate at which the subdomain where the viscous/vortical effects are of leading order shrinks in proportion to the overall size of the flow domain. This rate is proportional to $1/\sqrt{R_x}$ for laminar flow. The physics underlying this rate dictate important Reynolds number dependent properties, such as the growth of the boundary layer and the net viscous drag. The analysis herein exploits the similarity structure admitted by the relevant mean dynamical equation to estimate the analogous rate for the turbulent boundary layer, and to describe the operative physical processes.

Increases in Reynolds number are generically accompanied by a scale separation between the motions characteristic of the spatially coincident velocity and vorticity fields. In the laminar case, scale separation is reflected in the overall growth rate of δ. This is because (1) contains only two mechanisms, and thus the viscous force retains leading order across the entire boundary layer. In the turbulent case, the situation is more complicated. Here, purely inertial mechanisms constitute the leading order balance in the mean statement of dynamics over a significant and Reynolds number dependent portion of the boundary layer. About 50% of the mean vorticity exists on this domain, but this vorticity is on average confined, at any given instant, to a sub-volume of diminishing relative size. Owing to this, it is useful to conceptualize two possible ways that scale separation can occur in the turbulent boundary layer. One involves reducing the size of the vortical motions relative to the size of the velocity field motions upon which they are superposed. This can occur even if the physical size of the velocity field motions is also decreasing. The converse possibility involves small scale vortical motions being sparsely spread over a velocity field domain whose relative size is increasing. This can occur even if the physical size of the vortical motions is also increasing. As described herein, the distinction between these two similar scale separation scenarios becomes significant when considering the physical mechanisms associated with them.

The present effort seeks to describe the average rate at which the vorticity in the turbulent boundary layer concentrates onto a sub-volume of the overall flow domain. Toward this aim, theoretical analyses, as complemented/verified

by empirical observations, provide guidance [2]. One part of the resulting description uses the analysis of the mean dynamical equation directly to describe the scaling behaviors of a near-wall subdomain that accounts for about half of the mean vorticity integral. Another part exploits the self-similar behaviors exhibited by the mean and fluctuating vorticity, in concert with the under-appreciated fact that beyond the near-wall domain the $\tilde{\omega}_z$ bearing motions generally have an amplitude that greatly exceeds $|\Omega_z|$. This allows for an asymptotic description of the domain size that, at any given instant, contains the bulk of the outer region spanwise vorticity.

2. Similarity structure admitted by the mean momentum equation

The desired estimates are obtained through consideration of the self-similarities admitted by the mean momentum equation relevant to the problem of turbulent boundary layer flow over a flat plate. Under inner-normalization, this equation is given by

$$\left(U^+\frac{\partial U^+}{\partial x^+}+V^+\frac{\partial U^+}{\partial y^+}\right)-\frac{\partial T^+}{\partial y^+}=\frac{\partial^2 U^+}{\partial y^{+2}}. \tag{2}$$

While commonly called the Reynolds shear stress, $T^+=-\langle uv\rangle^+$ is in reality associated with the inertia of the turbulence. Three physical mechanisms are apparent in (2). Mean inertia (MI) is represented by the terms inside the parentheses on the left. The remaining term on the left is the mean effect of turbulent inertia (TI). The term on the right of (2) is the mean viscous force (VF). For purposes of describing the mechanisms underlying the TI term, there is use in the representation,

$$\frac{\partial T^+}{\partial y^+}=\langle v\omega_z\rangle^+-\langle w\omega_y\rangle^+, \tag{3}$$

which holds to within the boundary layer approximation. (Note that (3) is exact in channel flow.)

The terms in (2) exhibit distinct magnitude orderings on four layers. The scaling properties associated with these layers are summarized in table 1, e.g., see [2, 3, 4]. The ensuing section describes how these properties stem from a self-similar and continuous hierarchy of layers. Each layer on the hierarchy replicates the magnitude ordering of layer III, but as a function of scale. The hierarchy extends from near the bottom of layer II ($y^+\simeq 7$) to near the middle of layer IV ($y/\delta\simeq 0.5$). From (3) it is apparent that $\langle w\omega_y\rangle^+=\langle v\omega_z\rangle^+$ at the point where T^+ reaches a maximum, or equivalently, where the TI term has a positive to negative zero-crossing. Closer to the wall $\langle w\omega_y\rangle^+$ is larger, while farther from the wall $\langle v\omega_z\rangle^+$ is larger. The $\langle w\omega_y\rangle^+$ term is associated with change of scale effects caused by vorticity stretching, while the $\langle v\omega_z\rangle^+$ term is associated with advective transport [5].

Table 1. Magnitude ordering and scaling behaviors associated with the four layer structure of the mean momentum equation. Note that the layer IV properties are asymptotically attained as $\delta^+\to\infty$.

Physical layer	Magnitude ordering	Δy increment	ΔU increment
I	$\|\mathrm{MI}\|\simeq\|\mathrm{VF}\|\gg\|\mathrm{TI}\|$	$O(\nu/u_\tau)$ (≤ 3)	$O(u_\tau)$ (≤ 3)
II	$\|\mathrm{VF}\|\simeq\|\mathrm{TI}\|\gg\|\mathrm{MI}\|$	$O(\sqrt{\nu\delta/u_\tau})$ $(\simeq 1.6)$	$O(U_\infty)$ $(\simeq 0.5)$
III	$\|\mathrm{MI}\|\simeq\|\mathrm{VF}\|\simeq\|\mathrm{TI}\|$	$O(\sqrt{\nu\delta/u_\tau})$ $(\simeq 1.0)$	$O(u_\tau)$ $(\simeq 1)$
IV	$\|\mathrm{MI}\|\simeq\|\mathrm{TI}\|\gg\|\mathrm{VF}\|$	$O(\delta)$ $(\to 1)$	$O(U_\infty)$ $(\to 0.5)$

2.1. Synopsis of the Boundary Layer Analysis

The boundary layer analysis has analogy with the somewhat simpler case of channel flow [4]. Relative to fully developed channel flow, however, the boundary layer analysis is complicated by an $x-$dependence, and by the non-constancy of the profile of the MI term in (2) over $0\leq y\leq\delta$. For equilibrium boundary layer flows (2) is well-approximated by

$$\frac{d^2U^+}{dy^{+2}}+\frac{dT^+}{dy^+}+\varepsilon^2 b(y^+,\varepsilon)=0, \tag{4}$$

where $\varepsilon = 1/\sqrt{\delta^+} = \varepsilon(x^+)$, and $b = b(y^+, \varepsilon)$ [6, 7]. The unknown $O(1)$ function b is constrained such that $\int_0^{\delta^+} b dy^+ = O(\delta^+)$ for all ε. Given this, integration of (4) yields $\varepsilon^{-2}(x^+) = O(\delta^+)$. Thus, the function $b(y^+)$ predominantly describes the shape of the *MI* profile, and ε predominantly describes the Reynolds number variation of its amplitude.

Equation 4 admits an invariant form on each of a continuous hierarchy of internal scaling layers called the L_β hierarchy [2, 4]. Each L_β layer has a width that varies with wall-normal position. Thus, there is a corresponding layer width distribution, $W^+(y^+)$. The attributes of $W^+(y^+)$ derive from the leading order balance of all three terms in (2) as expressed by (9) under the stretched coordinates described by (8). The position and width of each member of the self-similar layer hierarchy is determined by the small positive parameter, β. The existence of the invariant form is exposed by using the transformation

$$T_\beta(y^+) = T^+(y^+) - T^*(\eta, \varepsilon) - \beta y^+, \tag{5}$$

where $\eta = \varepsilon^2 y^+ = O(y/\delta)$. Equation (5) effectively defines β. In (5) $T^*(\eta, \varepsilon)$ is the outer approximation to T^+,

$$T^* = \int_\eta^{\eta(\delta)} b(s, \varepsilon) ds, \tag{6}$$

where $\eta(\delta)$ denotes the value of $\eta = O(1)$ at $y = \delta$. Substitution of (5) into (4) yields

$$\frac{d^2U^+}{dy^{+2}} + \frac{dT^+}{dy^+} + \beta = 0, \tag{7}$$

which is of a form identical to that found for channel flow. From here, differential transformations,

$$dy^+ = \beta^{-1/2} d\hat{y}, \qquad dT^+ = \beta^{1/2} d\hat{T}, \qquad dU^+ = d\hat{U}, \tag{8}$$

yield the invariant form,

$$\frac{d^2U^+}{d\hat{y}^2} + \frac{d\hat{T}}{d\hat{y}} + 1 = 0, \tag{9}$$

of the differential force balance [2].

Equation 9 holds on each L_β layer [6, 7]. The differential transformations (8) that lead to (9) underlie the similarity solution demonstrated by Klewicki [8]. The underlying dynamical self-similarity is most succinctly expressed in terms of the scaled gradient of the mean effect of turbulent inertia. It states that the quantity

$$A(\beta) = -\frac{d^2\hat{T}_\beta}{d\hat{y}^2}(0) = -\beta^{-3/2}\frac{d^2T^+}{dy^{+2}} \tag{10}$$

becomes an $O(1)$ function on the L_β hierarchy [2]. Physically, (10) is a statement about the wall-normal flux of turbulent inertial force. It states that this flux approaches an invariant function when the width of each L_β layer is used as a characteristic length. On the portion of the L_β hierarchy interior to the outer edge of layer III ($y^+ \leq 2.6\varepsilon^{-1}$), $A(\beta)$ is an $O(1)$ but non-constant function. On the portion of the hierarchy outward of $y^+ \simeq 2.6\varepsilon^{-1}$, $A(\beta)$ approaches an $O(1)$ constant.

To within the boundary layer approximation, the relatively simpler form of the outer self-similarity leads to a closure of (2) on an interior domain that begins near the outer edge of layer III. The theory predicts that this is where logarithmic dependence is most rapidly emergent and accurately approximated in the mean velocity profile, e.g., [2]. Recent analysis of high Reynolds number boundary layer and pipe flow data support this prediction [9]. The existence of the underlying similarity solution on this subdomain can be demonstrated by directly integrating the closed equations between the relevant wall-normal limits. This is done, for example, by selecting the starting values from a direct numerical simulation (DNS) of the boundary layer, and subsequently comparing the similarity solution with the DNS solution. The analysis details pertaining to the construction of the boundary layer similarity solution are provided by Klewicki [8], and an example result for low δ^+ flow is given in figure 1.

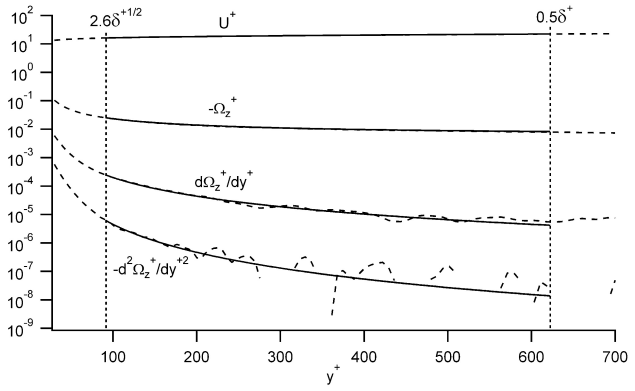

Fig. 1. Comparison of the inner-normalized profiles of U^+, Ω_z^+, $d\Omega_z^+/dy^+$, $d^2\Omega_z^+/dy^{2+}$ on the domain $2.6\sqrt{\delta^+} \le y^+ \le \delta^+/2$ as determined from the $\delta^+ = 1245$ boundary layer DNS of [10]; – – –, and similarity solution of (4), with starting values selected from the DNS; ——.

Analysis and comparison of velocity and vorticity spectra from laboratory and field studies indicates that on the part of the L_β hierarchy where the VF term in (2) is of leading order ($7 \le y^+ \le 2.6\varepsilon^{-1}$) the relevant vortical motions become smaller than those representative of the velocity field primarily owing to vorticity stretching. This is described as scale separation via spatial confinement [11]. Conversely, on the inertially dominated part of the hierarchy the primary scale separation mechanism is associated with the transport of concentrated vortical motions by turbulent advection. This is described as scale separation via spatial dispersion. In this regard, instantaneous particle image velocimetry measurements over the outer region of boundary layers provide evidence of large scale zones of nearly uniform momentum that are segregated by narrow *vortical fissures*. These features were first revealed in the study of Meinhart & Adrian [12], shown to have connection to packets of hairpin-like vortices by Adrian et al. [13], and described relative to the mechanisms of (3) by Priyadarshana et al. [13]. Consideration of the mean enstrophy equation provides additional support for the near-wall vorticity stretching mechanism, as does the dominance of the $\langle w\omega_y\rangle^+$ contributions to (3) in layer II. Similarly, the dominance of the $\langle v\omega_z\rangle^+$ in layer IV supports advective transport. Furthermore, the behavior of the $\langle v\omega_z\rangle^+$ profile clearly exhibits constancy in layer IV when normalized using u_τ and the characteristic layer width distribution, W, of the L_β hierarchy [14]. This reveals that the advective dispersion of the vortical fissures in layer IV is described by this distribution. Specifically, as $\delta^+ \to \infty$, the layer IV distribution of L_β layer widths increasingly gains linear proportionality with the distance from the wall [2]. This physically reflects the process by which the vortical fissures are spatially dispersed in layer IV.

3. Estimating the viscous/vortical domain

The scaling behaviors of the four layer structure described in table 1, along with the associated similarity structure admitted by (4), provide a basis for estimating the rate at which viscous/vortical effects are confined to a domain of diminishing size as $\delta^+ \to \infty$. In what follows, the regions $y^+ < 2.6\varepsilon^{-1}$ and $y^+ > 2.6\varepsilon^{-1}$ are considered separately.

3.1. Width of the domain where the VF term is of leading order ($y^+ < 2.6\varepsilon^{-1}$)

Useful results derive from the structure of the mean vorticity, $\Omega_z(y)$, profile. To within the boundary layer approximation, Ω_z, is given by $-\partial U/\partial y$. The integral of the Ω_z profile is equal to $-U_\infty$, or equivalently the total boundary layer circulation per unit length, Γ_∞. As indicated in table 1, the inner-normalized mean velocity increment (Γ^+) from the wall to the outer edge of layer III is approximately $0.5\Gamma_\infty^+ + 4$. This stems from the theoretical result that $|\Omega_z^+|\varepsilon^{-1} = 1$ at $\varepsilon y^+ = O(1)$ [4]. As exemplified by figure 2, this prediction is confirmed by the empirical observation that $|\Omega_z^+|\varepsilon^{-1} = 1$ at $\varepsilon y^+ \simeq 2.6$.

Thus, as $\delta^+ \to \infty$ a little more than 50% of the total circulation (per unit length) remains confined to the region $y^+ \le 2.6\varepsilon^{-1}$, with the remainder being spread over a layer IV that has a width that asymptotically approaches δ. The

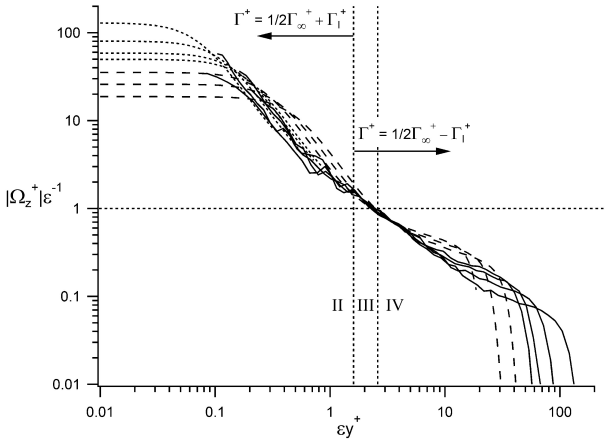

Fig. 2. Mean vorticity profiles in turbulent boundary layer flow, meso-normalized and plotted on logarithmic axes. Solid lines are from the experiments of [15]. Dashed lines is from the $\delta^+ = 671, 1034$, and 1245 simulations of [10]. Dotted lines are from the near-wall DNS, and have been transformed to correspond to the Reynolds numbers of the experimental profiles.

recognition that slightly more than $1/2$ of Γ_∞ resides within a domain that is $O(\varepsilon)$ provides the first part of the desired estimate. It also indicates that as $\delta^+ \to \infty$ the remainder of the circulation resides in the domain where the leading order mean dynamics are governed by the *MI* and *TI* terms in (2).

3.2. Volume occupied by the vortical motions in layer IV ($y^+ > 2.6\varepsilon^{-1}$)

It was previously noted that an especially relevant distinction between laminar and turbulent boundary layer structure is that the laminar flow equation (1) has only two operative mechanisms, while the mean dynamical equation for turbulent flow (2) has three. From this it is clear that the viscous force must be of leading order everywhere in the laminar boundary layer, and thus the growth rate of the boundary layer thickness itself is the quantity of interest. As just described, in an average sense only slightly more than $1/2$ of the total vorticity in the turbulent boundary layer resides in the region where the mean viscous force is of leading order. The rest of the vorticity is, on average, confined to a subdomain of layer IV.

The aim now is to gain an estimate for the size of this subdomain. To begin we note that with increasing distance from the wall the amplitude of the vorticity fluctuations rapidly exceeds that of Ω_z. For example, by $y^+ \simeq 40$ $\omega_z' = |\Omega_z|$, and by the outer edge of layer III $\omega_z'/|\Omega_z| \gg 1$, and increasingly so at this location as $\delta^+ \to \infty$ [14, 16]. This emergent behavior is exemplified (at low δ^+) in figure 3. As a result, the layer IV flow increasingly sees the regular appearance of both positive and negative instantaneous $\tilde{\omega}_z$ motions, with the mean becoming a diminishing *residual* of the interactions involving these instantaneous motions, e.g. [17]. An obvious additional consequence of this is that in layer IV $\tilde{\omega}_z$ is increasingly well-approximated by ω_z.

Via comparison it is apparent that the region where the fluctuations dominate the mean in figure 3 identically coincides with the region of approximately -1 power law dependence in figure 2. As described above, this also corresponds to layer IV, and thus the region of inertially dominated mean dynamics. Turbulent wall-flow dynamics are responsible for the outward wall-normal transport of mean vorticity, and simultaneously, the inward wall-normal transport of mean momentum [18]. Indeed, it can be formally shown that the mechanisms accomplishing this are the same [19]. From these considerations, and the fact that there are no vorticity sources internal to the present flow, one can readily surmise that the mean circulation contained in layer IV at any given streamwise position is derived from $\tilde{\omega}_z$ previously contained interior to $y/\delta = 2.6\varepsilon$. Existing evidence, up to $\delta^+ \simeq 1 \times 10^6$, indicates that much if not most of this vorticity is contained within the vortical fissures [14].

These observations immediately lead to an initial and conservative estimate that the transverse scale of the vortical fissures in layer IV are, on average, no wider than $2.6\varepsilon^{-1}$. Two primary factors underlie the further refinement of this

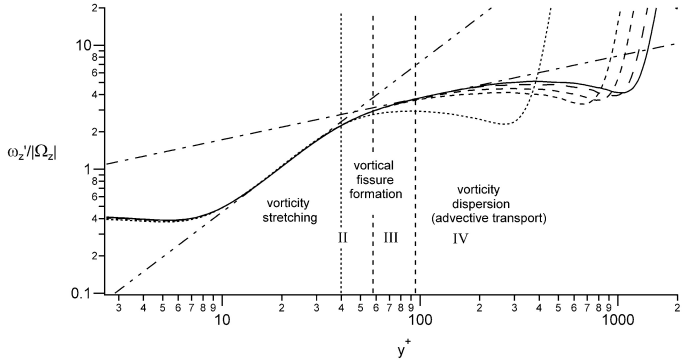

Fig. 3. Spanwise vorticity intensity profiles from the boundary layer DNS of [10], normalized by $|\Omega_z|$ and plotted versus y^+, $\delta^+ = 359$, · · ·; $\delta^+ = 830$, - - -; $\delta^+ = 974$, – – –; $\delta^+ = 1145$, — — —; and $\delta^+ = 1271$, ——. Vertical dashed lines denote the upper and lower boundaries of layer III at $\delta^+ = 1271$. Vertical dotted line denotes $y^+ = 40$, which is nominally where the exchange of mean enstrophy to fluctuating enstrophy (via vorticity stretching and reorientation) becomes negligible. Curve-fit in Layer II is given by $\omega_z'/|\Omega_z| = 0.027(y^+)^{1.21}$. Curve-fit in layer IV is given by $\omega_z'/|\Omega_z| = 0.796(y^+)^{0.34}$.

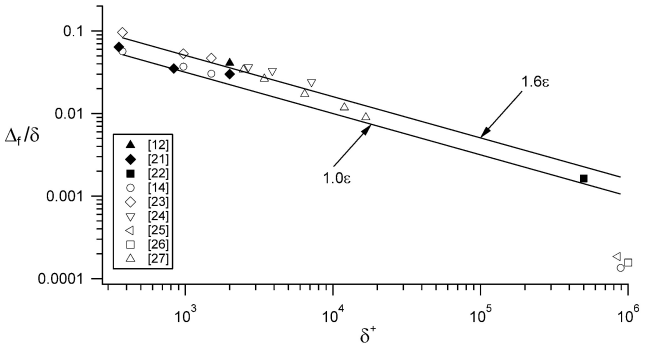

Fig. 4. Vortical fissure thickness estimates normalized by δ versus δ^+ (solid symbols). Streamwise Taylor microscale and ω_z advected lengths at $\varepsilon y^+ = 2.6$ (open symbols). Vortical fissure thicknesses from [12, 21, 22]. Taylor microscale and ω_z length scale measurements are from [14, 23, 24, 25, 26, 27].

upper bound. One comes from the scaling behaviors formally admitted by (2) that underlie the division of the mean circulation per unit length depicted in figure 2. Namely, from the wall to $y^+ \simeq 2.6\varepsilon^{-1}$ the $|\Omega_z|$ drops from u_τ^2/ν to $\sqrt{u_\tau^3/\nu\delta}$. From this point $|\Omega_z|$ drops to u_τ/δ by the upper end of the L_β hierarchy, and then decays approximately linearly to zero at $y = \delta$. The latter of these sets constraints on how much circulation can reside in a given number of fissures. (Note that number of uniform momentum zones and vortical fissures increases with δ^+ to account for the total vorticity content of layer IV. A second factor derives from the scaling behavior of Ω_z in the region $y^+ \leq 40$. The Ω_z profile exhibits a precipitous drop between $7 \leq y^+ \leq 40$. Analysis of the mean enstrophy equation indicates that this feature is associated with the exchange of mean-to-fluctuating enstrophy, and that this process universally scales on the inner length scale for all of the canonical wall-flows [14]. These attributes are reflected in figure 3.

From these considerations one can surmise that the widths of the fissures, Δ_f, are, on average, no less than the width of layer III, and no greater than the width of layer II, i.e., $1.0\varepsilon \leq \Delta_f/\delta \leq 1.6\varepsilon$. The data of figure 4 support this assertion. This figure presents direct quantifications of Δ_f/δ from boundary layer PIV measurements over the range $10^3 \leq \delta^+ \leq 10^6$, and shows that Δ_f/δ (solid symbols) fall within the expected range. The Taylor microscale and vorticity length scale data on this figure also provide evidence that as δ^+ increases the fissures develop an intermittent internal structure, while retaining the predicted $O(u_\tau)$ velocity increment across each fissure [14]. These structural features are also consistent with other recent observations in high Reynolds number flows, e.g., [20].

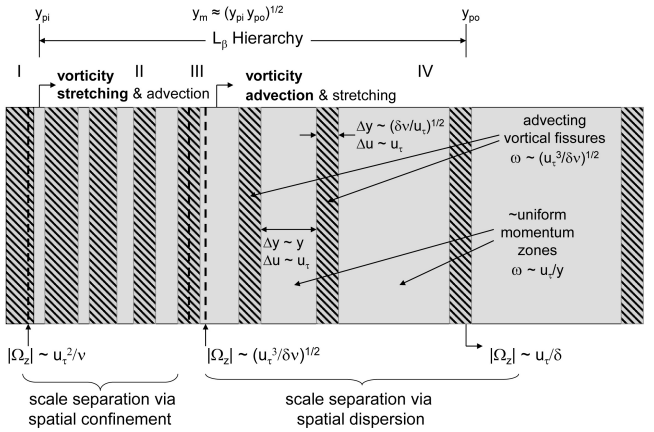

Fig. 5. Schematic depiction of the processes responsible for scale separation between the velocity and vorticity fields in turbulent wall-flows. The velocity field motions (light grey) are space-filling throughout the flow. The vorticity field motions (hatched regions) are confined to a sub-volume near the wall by vorticity stretching, and then the resulting fissures are dispersed by advective transport over the volume of layer IV, adapted from [14].

According to the present theory, the decay rate of $|\Omega_z|$ in the hierarchy portion of layer IV is predicted (in an order of magnitude sense) to cause a decrease from $|\Omega_z| \simeq u_\tau/\sqrt{\nu\delta/u_\tau}$ to $|\Omega_z| \simeq u_\tau/\delta$. When cast in this manner, it is apparent that the characteristic velocity increment remains u_τ, while the characteristic length increases from $\sqrt{\nu\delta/u_\tau}$ to δ. Thus, the logarithmic behavior of the mean velocity profile stems from the average linear increase of wall-normal distance between the vortical fissures with distance from the wall, as precisely reflected by linear increase of $W^+(y^+)$ in the lower portion of layer IV. As described previously [8, 18], this scaling behavior, and its underlying construction, has strongly correspondences with Townsend's *attached eddy* phenomenology, e.g., [28, 29]. In layer IV, the spatial dispersion via advective transport scale separation mechanism depicted in figure 5 is operative. The simplest prescription of this behavior assigns a single increment of u_τ to each fissure and uniform momentum zone. Under this prescription, about $1/2$ of the total circulation (per unit length) in layer IV is associated with the fissures. Existing evidence indicates, however, that while the typical velocity increment across a fissure is $O(u_\tau)$, the average value is greater than unity, with the associated increment across the uniform momentum zones being less than unity [12, 21]. It is physically rational to expect that the fissures will account for an even greater fraction as $\delta^+ \to \infty$.

4. Conclusions

The present aim is to obtain an estimate for the rate at which the domain containing the bulk of the vorticity in the turbulent boundary layer diminishes relative to overall size of the boundary layer, δ. The scaling properties associated with the decay rate of the mean vorticity, $|\Omega_z|$, indicate that, independent of the Reynolds number, δ^+, slightly more than half of total circulation per unit length, $|\Gamma_\infty|$, is contained within the domain in which the mean viscous force term in the mean dynamical equation is of leading order. Relative to δ, this domain has a thickness of approximately $2.6\varepsilon = 2.6/\sqrt{\delta^+}$.

In layer IV ($y^+ \geq 2.6\varepsilon^{-1}$), the viscous/vortical effects are, at any instant, confined to a subdomain of diminishing size such that the leading order mean dynamics only involve the terms representing mean and turbulent inertia. Based upon the analytically determined scaling behaviors of the Ω_z profile in layer IV, the apparent self-similarity between $\omega_z{}'$ (rms) and Ω_z, the dominance of the ω_z fluctuations relative to $|\Omega_z|$ in layer IV, and the empirically confirmed scaling behaviors for the vortical fissure widths, it can be surmised that the structure of layer IV is as depicted in figure 5. If a velocity increment of $1u_\tau$ is respectively assigned to each fissure and uniform momentum zone in this figure, then about 50% of the circulation (per unit length) in layer IV is confined to the fissures. Existing empirical evidence indicates that this is a conservative estimate [12, 21]. Physical considerations lead one to believe that actual value is in excess of 75% at low Reynolds number, and that this percentage increases with δ^+.

Given that the outer normalized vortical fissure widths also scale like $\varepsilon = 1/\sqrt{\delta^+}$, the above conservative estimate indicates at least 75% of Γ_∞ in the turbulent boundary layer resides within a domain of $C(\delta^+)\varepsilon$, where $C(\delta^+)$ is a Reynolds number dependent coefficient. Again, the actual value is probably more like 90% at low δ^+, and increases from there with further increments in Reynolds number. The value of C is always greater than about 7.8. This corresponds to a nascent four-layer regime boundary layer that has just two fissures (each having width $\simeq 1.3\varepsilon$, see figure 4) and two uniform momentum zones in layer IV; i.e., 2.6ε (layer III and below) + 2.6ε (two fissures) + 2.6ε (two uniform momentum zones). More significantly, the approximately logarithmic growth of $|\Gamma_\infty^+| = U_\infty^+$ with increasing δ^+ indicates that C also exhibits an approximately logarithmic increase. Thus, the domain containing the bulk of the net circulation diminishes relative to δ like $\sim \varepsilon\log(\varepsilon^{-2})$, or equivalently, $\log(\delta^+)/\sqrt{\delta^+}$.

The present theoretical formulation predicts that a logarithmic mean profile emerges most rapidly in the domain $2.6\sqrt{\delta^+} \leq y^+ \leq \delta^+/2$ [2, 30]. The primary elements of the instantaneous flow in this domain are uniform momentum zones segregated by narrow vortical fissures [12, 13]. The evidence presented herein indicates that the vortical fissures are of inner-normalized width $\simeq 1.3\sqrt{\delta^+}$. A logarithmic mean profile arises because the mean momentum equation admits the emerging self-similar structure that underlies the similarity solution demonstrated in figure 1 [8]. Recent analyses of the mean velocity profile and higher order moments of the u fluctuations at high Reynolds number provide additional support for the existence of a self-similar flow structure in this region [9, 31, 32]. The uniform momentum zone and vortical fissure description readily accounts for the emerging self-similarity between the mean and rms spanwise vorticity (figure 3), and is also likely to account for the self-similar behaviors observed in the u fluctuations.

Acknowledgements

The author is grateful to all of the researchers who made their data available for figures 1-4. This work was partially supported by the Australian Research Council.

References

[1] Schlichting H, Gersten K. Boundary Layer Theory. Berlin: Springer-Verlag; 2000.

[2] Fife P, Klewicki J, Wei T. Time averaging in turbulence settings may reveal an infinite hierarchy of length scales. J of Discrete and Continuous Dynamical Systems. 2009;24:781–807.

[3] Wei T, Fife P, Klewicki J, McMurtry P. Properties of the mean momentum balance in turbulent boundary layer, pipe and channel flows. J Fluid Mech. 2005;522:303–327.

[4] Fife P, Klewicki J, McMurtry P, Wei T. Stress gradient balance layers and scale hierarchies in wall-bounded turbulence. J Fluid Mech. 2005;532:165–189.

[5] Tennekes H, Lumley J. A First Course in Turbulence. Cambridge, MA: MIT Press; 1972.

[6] Metzger MM, Adams P, Fife P. Mean momentum balance in moderately favourable pressure gradient turbulent boundary layers. J Fluid Mech. 2008;617:107–140.

[7] Klewicki J, Ebner R, Wu X. Mean dynamics of transitional boundary layer flow. J Fluid Mech. 2011;682:617–651.

[8] Klewicki J. Self-similar mean dynamics in turbulent wall-flows. J Fluid Mech. 2013;718:596–621.

[9] Marusic I, Monty J, Hultmark M, Smits A. On the logarithmic region in wall turbulence. J Fluid Mech. 2013;716:R3.

[10] Schlatter P, Orlu R. Assessment of direct numerical simulation data of turbulent boundary layers. J Fluid Mech. 2010;659:116–126.

[11] Morrill-Winter C, Klewicki J. Influences of boundary layer scale separation on the vorticity transport contribution to turbulent inertia. Phys Fluids. 2013;25:015108.

[12] Meinhart C, Adrian RJ. On the existence of uniform momentum zones in turbulent boundary layers. Phys Fluids. 1995;7:694–696.

[13] Adrian R, Meinhart C, Tomkins C. Vortex organization in the outer region of the turbulent boundary layer. J Fluid Mech. 2000;422:1–54.

[14] Priyadarshana P, Klewicki J, Treat S, Foss J. Statistical structure of turbulent boundary layer velocity-vorticity products at high and low Reynolds numbers. J Fluid Mech. 2007;570:307–346.

[15] Klewicki J. A description of turbulent wall-flow vorticity consistent with mean dynamics. J Fluid Mech. 2013;(under review).

[16] Hutchins N, Nickles T, Marusic I, Chong M. Hot-wire spatial resolution issues in wall-bounded turbulence. J Fluid Mech. 2009;635:103–136.

[17] Klewicki J. Self-sustaining traits of the near-wall motions underlying boundary layer stress transport. In: Panton R, editor. Self-Sustaining Mechanisms of Wall Turbulence. Ashurst Lodge, Southampton: Computational Mechanics Publications; 1997. p. 136–166.

[18] Klewicki J, Gendrich C, Foss J, Falco R. On the sign of the instantaneous spanwise vorticity component in the wall region of a turbulent boundary layer. Phys Fluids A. 1990;2:1497–1500.

[19] Klewicki J, Fife P, Wei T, McMurtry P. A physical model of the turbulent boundary layer consonant with mean momentum balance structure. Phil Trans Roy Soc A. 2007;365:823–839.

[20] Eyink G. Turbulent flow in pipes and channels as cross-stream "inverse cascades" of vorticity. Phys Fluids. 2008;20:125101.

[21] Hunt J, Eames I, Da Silva C, Westerweel J. Interfaces and inhomogeneous turbulence. Phil Trans Roy Soc A. 2011;369:811–832.

[22] Morris S S Stolpa, Slaboch P, Klewicki J. Near-surface particle image velocimetry measurements in a transitionally rough-wall atmospheric boundary layer. J Fluid Mech. 2007;580:319–338.

[23] Klewicki J, Falco R. On accurately measuring statistics associated with small-scale structure in turbulent boundary layers using hot-wire probes. J Fluid Mech. 1990;219:119–142.

[24] Stanislas M, Perret L, Foucalt J. Vortical structures in the turbulent boundary layer: A possible route to a universal representation. J Fluid Mech. 2008;602:327–382.

[25] Metzger M. Length and time scales of the near-surface axial velocity in a high Reynolds number turbulent boundary layer. Int J Heat and Fluid Flow. 2006;27:534–541.

[26] Klewicki J, Priyadarshana P, Metzger M. Statistical structure of the fluctuating wall-pressure and its in-plane gradients at high Reynolds number. J Fluid Mech. 2008;609:195–220.

[27] Marusic I, Adrian R. The eddies and scales of wall turbulence. In: Davidson P, Kaneda Y, Sreenivasan K, editors. Ten Chapters in Turbulence. Cambridge: Cambridge University Press; 2013. p. 176–220.

[28] Perry A, Chong M. On the mechanism of wall turbulence. J Fluid Mech. 1982;119:173–217.

[29] Perry A, Marusic I. A wall-wake model for the turbulence structure of boundary layers. Part 1. Extension of the attached eddy hypothesis. J Fluid Mech. 1995;298:361–388.

[30] Klewicki J, Fife P, Wei T. On the logarithmic mean profile. J Fluid Mech. 2009;638:73–93.

[31] Tsuji Y, Lindgren B, Johansson AV. Self-similar profile of probability density functions in zero-pressure gradient turbulent boundary layers. Fluid Dyn Res. 2005;37:293–316.

[32] Meneveau C, Marusic I. Generalized logarithmic law for high-order moments in turbulent boundary layers. J Fluid Mech. 2013;719:R1.